New Escape Probabilities and Treatment of Molecular Shielding

(c) Peter Woitke, October 2022

The currently used escape probability method in ProDiMo, which enters the non-LTE rate equations and the calculation of the line heating/cooling rates, is based on Eq. (73) in Woitke et al. (2009), which is a rather crude approximation as it only considers radiative pumping by continuum photons in the radial direction, and line photon escape into the upward vertical direction. In particular, the IR-pumping from the disc below is incorrectly attenuated by the radial line optical depth $\tau_{ul}^{\rm rad}$, which can be huge, i.e. we are likely underestimating the true IR pumping. In addition, in the outer optically thin disc regions, the escape probability is currently limited to $P_{ul}^{\rm esc} \le \frac{1}{2}$, where it should be $P_{ul}^{\rm esc} \to 1$.

This document presents a new idea how to calculate the line averaged mean intensity ("J-bar") more rigorously by taking into account continuum radiative transfer effects in the resonance region

$$\bar{J}_{ul} = \frac{1}{4\pi} \iint \phi_\nu \, I_\nu(\vec{n}) \, d\Omega \, d\nu \ , \tag{1}$$

where ϕ_ν is the line profile function associated with the spectral line $u \to l$ and I_ν is the spectral intensity. We will show that, by making some assumptions about disc geometry and locality of radiative transfer quantities explained below, it is possible to arrive at a final expression that reads again

$$\bar{J}_{ul} = P_{ul}^{\rm pump} J_\nu^{\rm cont} + (1 - P_{ul}^{\rm esc}) S_{\rm L} \tag{2}$$

but now with new $P_{ul}^{\rm pump}$ and $P_{ul}^{\rm esc}$ that depend not only on line optical depths, but also on continuum optical depths, and take into account pumping from and escape into all directions. $S_{\rm L}$ is the line source function and $J_\nu^{\rm cont}$ the continuous mean intensity that would result if the line has zero opacity.

1 The new escape probability method

We write the line & continuum radiative transfer equation as

$$\frac{dI_\nu}{ds} = -(\kappa_{\rm C} + \kappa_{\rm L}\phi_\nu) I_\nu \ + \ \kappa_{\rm C} S_{\rm C} \ + \ \kappa_{\rm L} \phi_\nu S_{\rm L} \tag{3}$$

where the continuum, absorption and scattering opacities [$\rm cm^{-1}$], and the continuum source function, assuming isotropic scattering, are given by

$$\kappa_{\rm C} \ = \ \kappa_\nu^{\rm abs} + \kappa_\nu^{\rm sca} \ , \tag{4}$$

$$\kappa_{\rm C} \, S_{\rm C} \ = \ \kappa_\nu^{\rm abs} B_\nu(T_{\rm d}) + \kappa_\nu^{\rm sca} J_\nu^{\rm cont} \ . \tag{5}$$

The line opacity [$\rm cm^{-1}\,Hz$], Gaussian line profile function [$\rm Hz^{-1}$], and line source function [$\rm erg\,cm^{-2}\,s^{-1}\,Hz^{-1}\,sr^{-1}$] are given by

$$\kappa_{\rm L} \ = \ \frac{h\nu_{ul}}{4\pi} \big(n_l B_{lu} - n_u B_{ul} \big) \ , \tag{6}$$

$$\phi_\nu \ = \ \frac{1}{\sqrt{\pi}\Delta\nu_{\rm D}} \, {\rm e}^{-\left(\frac{\nu-\nu_{ul}}{\Delta\nu_{\rm D}}\right)^2} \ , \tag{7}$$

$$S_{\rm L} \ = \ \frac{2h\nu_{ul}^3}{c^2} \left(\frac{g_u \, n_l}{g_l \, n_u} - 1 \right)^{-1} \ , \tag{8}$$

where ν_{ul} is the line centre frequency, $\nu_{\rm D} = \nu_{ul} \, \Delta v / c$ the Doppler width and $\Delta v = \sqrt{v_{\rm th}^2 + v_{\rm turb}^2}$ the line width in velocity space. Introducing the optical depth and maximum optical depth as

$$t_\nu(s) \ = \ \int_0^s \kappa_{\rm C} + \kappa_{\rm L}\phi_\nu \, ds \ , \tag{9}$$

$$\tau_\nu \ = \ t_\nu(s_{\rm max}) \ , \tag{10}$$

the formal solution of Eq. (3) is

$$I_\nu(\vec{n}) = I_\nu^0(\vec{n})\ \mathrm{e}^{-\tau_\nu} + \int_0^{s_\mathrm{max}} (\kappa_\mathrm{C} S_\mathrm{C} + \kappa_\mathrm{L}\phi_\nu S_\mathrm{L})\ \mathrm{e}^{-t_\nu}\, ds\ , \tag{11}$$

where $\vec{n}$ is the direction of the ray (unit vector) and s_max is the distance backward along the ray up to the point where the ray enters the model volume. $I_\nu^0(\vec{n})$ is the incident intensity at that point in direction $\vec{n}$.

Assumption 1 (locality): We assume that all radiative transfer properties, that is κ_C, κ_L, S_L, S_C and ϕ_ν, are independent of location and direction, and given by their local values. Assuming $S_\mathrm{L} = \mathrm{const}$ is standard in escape probability theory, because the line photons typically interact only within a small "resonance volume" around the point of interest. Generalising this idea to the continuum transfer properties is a new idea (however, see Hummer & Rybicki 1985).

This way, we try to capture the most relevant continuum radiative transfer effects in that resonance region, where there is a competition between line and continuum photons. Constant ϕ_ν also means that we neglect velocity line shifts, i.e. we assume a static medium. The only quantities that are allowed to depend on direction are $I_\nu^0(\vec{n})$ and s_max (and hence τ_ν). In this case the formal solution of the RT equation (11) simplifies to

$$I_\nu(\vec{n}) = I_\nu^0(\vec{n})\ \mathrm{e}^{-\tau_\mathrm{C}-\tau_\mathrm{L}\phi_\nu} + \frac{\tau_\mathrm{C} S_\mathrm{C} + \tau_\mathrm{L}\phi_\nu S_\mathrm{L}}{\tau_\mathrm{C} + \tau_\mathrm{L}\phi_\nu}\left(1 - \mathrm{e}^{-\tau_\mathrm{C}-\tau_\mathrm{L}\phi_\nu}\right)\ , \tag{12}$$

where we have used the continuum and line centre optical depths $\tau_\mathrm{C} = \kappa_\mathrm{C} s_\mathrm{max}$ and $\tau_\mathrm{L} = \kappa_\mathrm{L} s_\mathrm{max}$.

Assumption 2 (disc geometry): We consider three major directions: radial (the rays coming from the stellar surface – often important for pumping), vertically upwards and vertically downwards. At a given location in the disc, the star occupies a small solid angle $\Omega_\star$. The other two principle directions cover half of $\Omega_\mathrm{d} = 4\pi - \Omega_\star$ each. All rays coming from the stellar surface are represented by a single radial ray. For the upward and downward directions, we approximate the disc as being plane-parallel with $\mu = \cos(\theta)$ where θ is the angle with the vertical. Thus we find from Eq. (1)

$$\bar{J}_{ul} = \frac{\Omega_\star}{4\pi}\int \phi_\nu\, I_\nu^\mathrm{rad}\, d\nu + \frac{\Omega_\mathrm{d}}{8\pi}\int \phi_\nu \int_0^1 I_\nu(\mu)\, d\mu\, d\nu + \frac{\Omega_\mathrm{d}}{8\pi}\int \phi_\nu \int_{-1}^0 I_\nu(\mu)\, d\mu\, d\nu\ . \tag{13}$$

Introducing the vertically upwards and downwards (accross the disc) line and continuum optical depths, $\tau_\mathrm{L}^\uparrow$, $\tau_\mathrm{L}^\downarrow$, $\tau_\mathrm{C}^\uparrow$ and $\tau_\mathrm{C}^\downarrow$, respectively, and the radially inward line and continuum optical depths, $\tau_\mathrm{L}^\mathrm{rad}$ and $\tau_\mathrm{C}^\mathrm{rad}$, and using plane-parallel geometry $\tau(\mu) = \tau(\mu=0)/\mu$ we obtain from Eqs. (12) and (13)

$$\bar{J}_{ul} = \frac{\Omega_\star}{4\pi}\int \phi_\nu \left(I_\nu^\star\, \mathrm{e}^{-\tau_\mathrm{C}^\mathrm{rad}-\tau_\mathrm{L}^\mathrm{rad}\phi_\nu} + \frac{\tau_\mathrm{C}^\mathrm{rad} S_\mathrm{C} + \tau_\mathrm{L}^\mathrm{rad}\phi_\nu S_\mathrm{L}}{\tau_\mathrm{C}^\mathrm{rad} + \tau_\mathrm{L}^\mathrm{rad}\phi_\nu}\left(1 - \mathrm{e}^{-\tau_\mathrm{C}^\mathrm{rad}-\tau_\mathrm{L}^\mathrm{rad}\phi_\nu}\right)\right) d\nu \tag{14}$$

$$+ \frac{\Omega_\mathrm{d}}{8\pi}\int \phi_\nu \int_0^1 I_\nu^\mathrm{ISM}\, \mathrm{e}^{-\frac{\tau_\mathrm{C}^\uparrow}{\mu}-\frac{\tau_\mathrm{L}^\uparrow}{\mu}\phi_\nu} + \frac{\tau_\mathrm{C}^\uparrow S_\mathrm{C} + \tau_\mathrm{L}^\uparrow\phi_\nu S_\mathrm{L}}{\tau_\mathrm{C}^\uparrow + \tau_\mathrm{L}^\uparrow\phi_\nu}\left(1 - \mathrm{e}^{-\frac{\tau_\mathrm{C}^\uparrow}{\mu}-\frac{\tau_\mathrm{L}^\uparrow}{\mu}\phi_\nu}\right) d\mu\, d\nu \tag{15}$$

$$+ \frac{\Omega_\mathrm{d}}{8\pi}\int \phi_\nu \int_{-1}^0 I_\nu^\mathrm{ISM}\, \mathrm{e}^{-\frac{\tau_\mathrm{C}^\downarrow}{|\mu|}-\frac{\tau_\mathrm{L}^\downarrow}{|\mu|}\phi_\nu} + \frac{\tau_\mathrm{C}^\downarrow S_\mathrm{C} + \tau_\mathrm{L}^\downarrow\phi_\nu S_\mathrm{L}}{\tau_\mathrm{C}^\downarrow + \tau_\mathrm{L}^\downarrow\phi_\nu}\left(1 - \mathrm{e}^{-\frac{\tau_\mathrm{C}^\downarrow}{|\mu|}-\frac{\tau_\mathrm{L}^\downarrow}{|\mu|}\phi_\nu}\right) d\mu\, d\nu\ . \tag{16}$$

Introducing the second exponential integral function $E_2(\tau) = \int_0^1 \exp\left(-\frac{\tau}{\mu}\right) d\mu$ we find

$$\bar{J}_{ul} = \frac{\Omega_\star}{4\pi} \int \phi_\nu \left(I_\nu^\star \, \mathrm{e}^{-\tau_\mathrm{C}^\mathrm{rad} - \tau_\mathrm{L}^\mathrm{rad}\phi_\nu} + \frac{\tau_\mathrm{C}^\mathrm{rad} S_\mathrm{C} + \tau_\mathrm{L}^\mathrm{rad}\phi_\nu S_\mathrm{L}}{\tau_\mathrm{C}^\mathrm{rad} + \tau_\mathrm{L}^\mathrm{rad}\phi_\nu} \left(1 - \mathrm{e}^{-\tau_\mathrm{C}^\mathrm{rad} - \tau_\mathrm{L}^\mathrm{rad}\phi_\nu}\right) \right) d\nu \tag{17}$$

$$+ \frac{\Omega_\mathrm{d}}{8\pi} \int \phi_\nu \left(I_\nu^\mathrm{ISM} \, E_2(\tau_\mathrm{C}^\uparrow + \tau_\mathrm{L}^\uparrow\phi_\nu) + \frac{\tau_\mathrm{C}^\uparrow S_\mathrm{C} + \tau_\mathrm{L}^\uparrow\phi_\nu S_\mathrm{L}}{\tau_\mathrm{C}^\uparrow + \tau_\mathrm{L}^\uparrow\phi_\nu} \left(1 - E_2(\tau_\mathrm{C}^\uparrow + \tau_\mathrm{L}^\uparrow\phi_\nu)\right) \right) d\nu \tag{18}$$

$$+ \frac{\Omega_\mathrm{d}}{8\pi} \int \phi_\nu \left(I_\nu^\mathrm{ISM} \, E_2(\tau_\mathrm{C}^\downarrow + \tau_\mathrm{L}^\downarrow\phi_\nu) + \frac{\tau_\mathrm{C}^\downarrow S_\mathrm{C} + \tau_\mathrm{L}^\downarrow\phi_\nu S_\mathrm{L}}{\tau_\mathrm{C}^\downarrow + \tau_\mathrm{L}^\downarrow\phi_\nu} \left(1 - E_2(\tau_\mathrm{C}^\downarrow + \tau_\mathrm{L}^\downarrow\phi_\nu)\right) \right) d\nu \, , \tag{19}$$

where $I_\nu^\star$ and I_ν^ISM are the stellar and interstellar incident intensities, respectively. We now introduce the dimensionless profile function $\phi(x) = \exp(-x^2)/\sqrt{\pi}$ with $x = (\nu - \nu_{ul})/\Delta\nu_\mathrm{D}$ and six basic 2D-functions, which all produce values between 0 and 1, to further simplify the result

$$\alpha_0(\tau_\mathrm{L}, \tau_\mathrm{C}) = \int \phi(x) \, \mathrm{e}^{-\tau_\mathrm{C} - \tau_\mathrm{L}\phi(x)} \, dx \, , \tag{20}$$

$$\alpha_1(\tau_\mathrm{L}, \tau_\mathrm{C}) = \int \phi(x) \, \frac{\tau_\mathrm{C}}{\tau_\mathrm{C} + \tau_\mathrm{L}\phi(x)} \left(1 - \mathrm{e}^{-\tau_\mathrm{C} - \tau_\mathrm{L}\phi(x)}\right) dx \, , \tag{21}$$

$$\alpha_2(\tau_\mathrm{L}, \tau_\mathrm{C}) = \int \phi(x) \, \frac{\tau_\mathrm{L}\phi(x)}{\tau_\mathrm{C} + \tau_\mathrm{L}\phi(x)} \left(1 - \mathrm{e}^{-\tau_\mathrm{C} - \tau_\mathrm{L}\phi(x)}\right) dx \, , \tag{22}$$

$$\beta_0(\tau_\mathrm{L}, \tau_\mathrm{C}) = \int \phi(x) \, E_2\big(\tau_\mathrm{C} + \tau_\mathrm{L}\phi(x)\big) \, dx \, , \tag{23}$$

$$\beta_1(\tau_\mathrm{L}, \tau_\mathrm{C}) = \int \phi(x) \, \frac{\tau_\mathrm{C}}{\tau_\mathrm{C} + \tau_\mathrm{L}\phi(x)} \left(1 - E_2\big(\tau_\mathrm{C} + \tau_\mathrm{L}\phi(x)\big)\right) dx \, , \tag{24}$$

$$\beta_2(\tau_\mathrm{L}, \tau_\mathrm{C}) = \int \phi(x) \, \frac{\tau_\mathrm{L}\phi(x)}{\tau_\mathrm{C} + \tau_\mathrm{L}\phi(x)} \left(1 - E_2\big(\tau_\mathrm{C} + \tau_\mathrm{L}\phi(x)\big)\right) dx \, , \tag{25}$$

where, using the Einstein relations, from now on

$$\tau_\mathrm{L} = \int \frac{\kappa_\mathrm{L}}{\Delta\nu_\mathrm{D}} \, ds = \int \frac{h\nu_{ul}}{4\pi \, \Delta\nu_\mathrm{D}} \big(n_l B_{lu} - n_u B_{ul}\big) \, ds = \int \frac{A_{ul}}{8\pi \, \Delta v} \Big(\frac{c}{\nu_{ul}}\Big)^3 \big(n_l \frac{g_u}{g_l} - n_u\big) \, ds \, . \tag{26}$$

The results are

$$\begin{aligned} \bar{J}_{ul} = {} & \tfrac{\Omega_\star}{4\pi}\Big(I_\nu^\star \, \alpha_0(\tau_\mathrm{L}^\mathrm{rad}, \tau_\mathrm{C}^\mathrm{rad}) + S_\mathrm{C} \, \alpha_1(\tau_\mathrm{L}^\mathrm{rad}, \tau_\mathrm{C}^\mathrm{rad}) + S_\mathrm{L} \, \alpha_2(\tau_\mathrm{L}^\mathrm{rad}, \tau_\mathrm{C}^\mathrm{rad})\Big) \\ & + \tfrac{\Omega_\mathrm{d}}{8\pi}\Big(I_\nu^\mathrm{ISM} \, \beta_0(\tau_\mathrm{L}^\uparrow, \tau_\mathrm{C}^\uparrow) + S_\mathrm{C} \, \beta_1(\tau_\mathrm{L}^\uparrow, \tau_\mathrm{C}^\uparrow) + S_\mathrm{L} \, \beta_2(\tau_\mathrm{L}^\uparrow, \tau_\mathrm{C}^\uparrow)\Big) \\ & + \tfrac{\Omega_\mathrm{d}}{8\pi}\Big(I_\nu^\mathrm{ISM} \, \beta_0(\tau_\mathrm{L}^\downarrow, \tau_\mathrm{C}^\downarrow) + S_\mathrm{C} \, \beta_1(\tau_\mathrm{L}^\downarrow, \tau_\mathrm{C}^\downarrow) + S_\mathrm{L} \, \beta_2(\tau_\mathrm{L}^\downarrow, \tau_\mathrm{C}^\downarrow)\Big) \, . \end{aligned} \tag{27}$$

From this geometric model we also get a prediction of the continuum, i.e. the mean intensity at line centre frequency as would be present if the line opacity was zero

$$\begin{aligned} J_\nu^\mathrm{cont} = {} & \tfrac{\Omega_\star}{4\pi}\Big(I_\nu^\star \, \alpha_0(0, \tau_\mathrm{C}^\mathrm{rad}) + S_\mathrm{C} \, \alpha_1(0, \tau_\mathrm{C}^\mathrm{rad})\Big) \\ & + \tfrac{\Omega_\mathrm{d}}{8\pi}\Big(I_\nu^\mathrm{ISM} \, \beta_0(0, \tau_\mathrm{C}^\uparrow) + S_\mathrm{C} \, \beta_1(0, \tau_\mathrm{C}^\uparrow)\Big) \\ & + \tfrac{\Omega_\mathrm{d}}{8\pi}\Big(I_\nu^\mathrm{ISM} \, \beta_0(0, \tau_\mathrm{C}^\downarrow) + S_\mathrm{C} \, \beta_1(0, \tau_\mathrm{C}^\downarrow)\Big) \, . \end{aligned} \tag{28}$$

Equation (28) is used to determine S_C. This means that we can calibrate S_C in such a way that our simple 3-way RT model with constant quantities results in the correct J_ν^cont as known from the proper solution of the continuum ratiave transfer problem. This is a great advantage as it allows us to eliminate most the principle problems coming with that simplified 3-way RT model in the continuum.

Comparing Eq. (27) to Eq. (2) we find the definitions of our new pumping and escape probabilities

$$P_{ul}^{\rm pump} = \frac{1}{J_\nu^{\rm cont}}\left(\frac{\Omega_\star}{4\pi}\left[I_\nu^\star\,\alpha_0(\tau_{\rm L}^{\rm rad},\tau_{\rm C}^{\rm rad}) + S_{\rm C}\,\alpha_1(\tau_{\rm L}^{\rm rad},\tau_{\rm C}^{\rm rad})\right] + \frac{\Omega_{\rm d}}{8\pi}\left[I_\nu^{\rm ISM}\left(\beta_0(\tau_{\rm L}^{\uparrow},\tau_{\rm C}^{\uparrow}) + \beta_0(\tau_{\rm L}^{\downarrow},\tau_{\rm C}^{\downarrow})\right) + S_{\rm C}\left(\beta_1(\tau_{\rm L}^{\uparrow},\tau_{\rm C}^{\uparrow}) + \beta_1(\tau_{\rm L}^{\downarrow},\tau_{\rm C}^{\downarrow})\right)\right]\right)\,, \quad (29)$$

$$P_{ul}^{\rm esc} = 1 - \frac{\Omega_\star}{4\pi}\alpha_2(\tau_{\rm L}^{\rm rad},\tau_{\rm C}^{\rm rad}) - \frac{\Omega_{\rm d}}{8\pi}\left(\beta_2(\tau_{\rm L}^{\uparrow},\tau_{\rm C}^{\uparrow}) + \beta_2(\tau_{\rm L}^{\downarrow},\tau_{\rm C}^{\downarrow})\right)\,. \quad (30)$$

The interpretation of these results is as follows:

- $P_{ul}^{\rm pump}$ is the *probability that continuum photons make it to the considered point*, given the presence of line opacity. The average is taken over all continuum photons that would contribute to $J_\nu^{\rm cont}$ when the line was not existing, whether they have been emitted by the star or by any point in the disc, averaged over the local line profile function.
- $P_{ul}^{\rm esc}$ is the *probability that line photons emitted anywhere in the disc, in the direction of the considered point, do not make it to the considered point*, averaged over the local line profile function. $P_{ul}^{\rm esc} < 1$ means that these line photons are either re-absorbed by line opacity, or re-absorbed/scattered by continuum opacity along the path to the considered point.

Since the order of photon emission & re-absorption and the optical depths effects along the photon paths can be reversed, $P_{ul}^{\rm esc}$ can also be interpreted as *the probability of a line photon emitted from the considered point not to have another line interaction in the disc*. It is important to realise the emphasis on further line interaction here. $P_{ul}^{\rm esc}$ is **not** the probability of line photons to escape the disc! That interpretation is only correct when there is no continuum opacity. Continuum opacity will prevent further line interaction, so it increases $P_{ul}^{\rm esc}$. The latter could be interpreted as "intrinsic escape", meaning that, once a line photon is absorbed and re-emitted by the dust, that continuum photon will escape the disc somehow, but this is actually not what the equations tell us. In particular, in the optically thick limiting case with $\tau_{\rm L} \ll \tau_{\rm C}$, the result is $P_{ul}^{\rm esc} \to 1$ and $P_{ul}^{\rm pump} \to 1$.

1.1 Practical computations

In practise, the six basic 2D-functions $\alpha_0(\tau_{\rm L},\tau_{\rm C}) \ldots \beta_2(\tau_{\rm L},\tau_{\rm C})$ are precalculated and then interpolated in 2D-tables. $I_\nu^\star$ and $I_\nu^{\rm ISM}$ are known functions, and $\tau_{\rm C}^{\rm rad}$, $\tau_{\rm C}^{\uparrow}$ and $\tau_{\rm C}^{\downarrow}$ are available after the initialisation of the disc structure and opacities in ProDiMo, which allows us to determine $S_{\rm C}$ from Eq. (28) at any point and frequency. The centre line optical depths $\tau_{\rm L}^{\rm rad}$ and $\tau_{\rm L}^{\uparrow}$ are integrated during the downward/outward sweep of the chemistry and heating/cooling balance in ProDiMo, just as before, but we also need $\tau_{\rm L}^{\downarrow}$ here, which requires another assumption.

Assumption 3 (downward line optical depths): We calculate $\tau_{\rm L}^{\downarrow}$ by assuming that (a) the line/continuum opacity ratio is the same for the upward and downward rays

$$\text{(a) using } \tau\text{-ratio} \qquad \tau_{\rm L}^{\downarrow} = \tau_{\rm C}^{\downarrow}\,\frac{\tau_{\rm L}^{\uparrow}}{\tau_{\rm C}^{\uparrow}} \quad (31)$$

$$\text{(b) using local } \kappa\text{-ratio} \quad \tau_{\rm L}^{\downarrow} = \tau_{\rm C}^{\downarrow}\,\frac{\kappa_{\rm L}}{\kappa_{\rm C}}\,. \quad (32)$$

or (b) using the local line/continuum opacity ratio. One could try other approximations here, or use information from a previous disc iteration if required.

1.2 Comparison to the old escape probability method

The old escape probability method in ProDiMo was based on

$$P_{ul}^{\mathrm{pump,old}} = \int \phi(x)\, \mathrm{e}^{-\tau_{\mathrm{L}}^{\mathrm{rad}}\phi(x)}\, dx \ , \tag{33}$$

$$P_{ul}^{\mathrm{esc,old}} = \frac{1}{2}\int \phi(x)\, E_2\big(\tau_{\mathrm{L}}^{\uparrow}\phi(x)\big)\, dx \ . \tag{34}$$

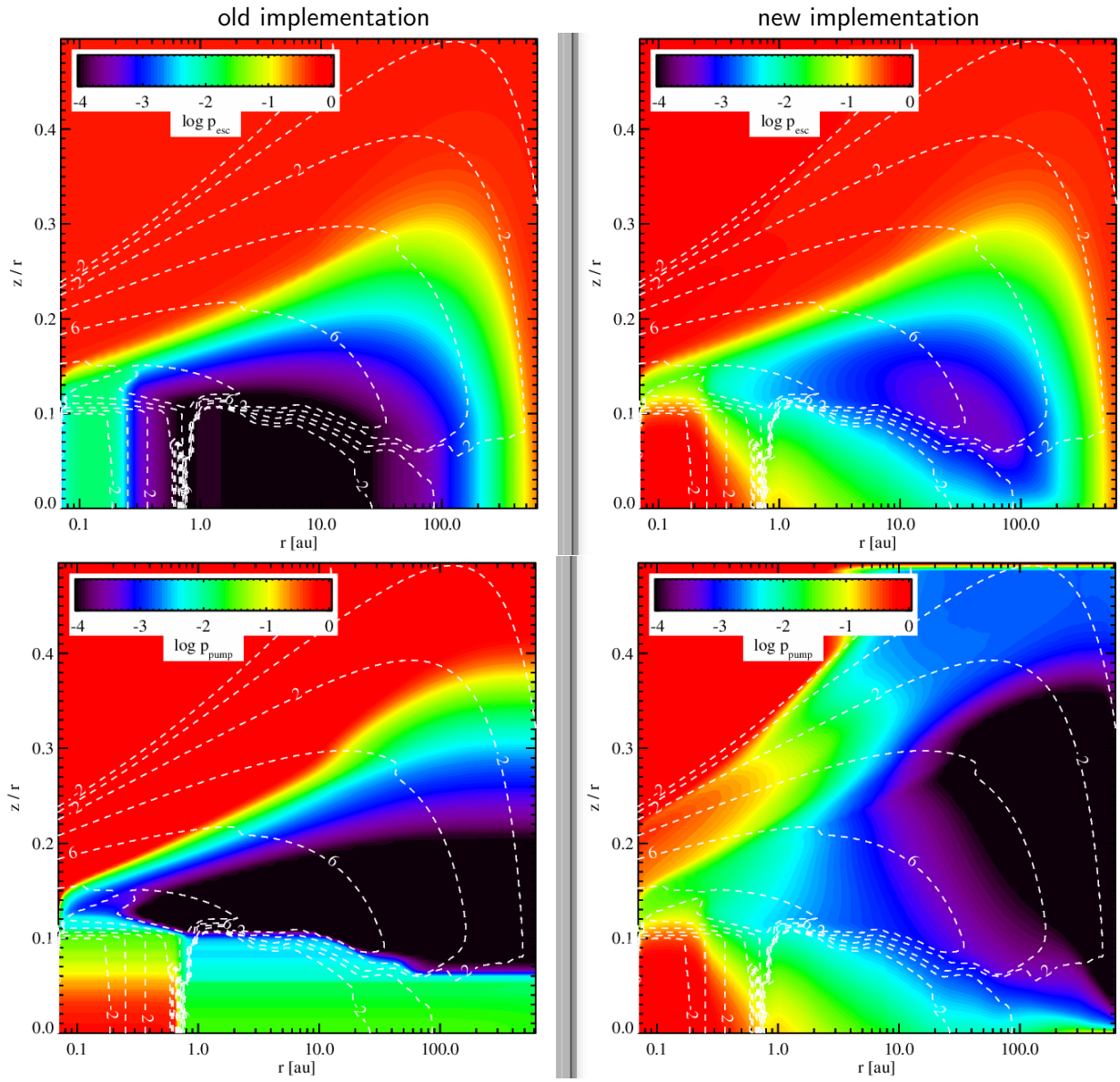

Figure 1: Escape probability (P_{ul}^{esc}, top) and continuuum pumping probability (P_{ul}^{pump}, bottom) of the OI 63 μm line in the ProDiMo standard T Tauri model. Left and right plots show the previous and new implementation of escape probability theory. The white dashed contours show the particle density of atomic oxygen $\log n_{\mathrm{OI}}[\mathrm{cm}^{-3}] = \{8, 6, 4, 2, 0, -2\}$

We can identify two cases where the new and old method have the same results.

1. If the stellar illumination dominates we have

$$\begin{aligned} J_\nu^{\rm cont} &= \frac{\Omega_\star}{4\pi} I_\nu^\star \, {\rm e}^{-\tau_{\rm C}^{\rm rad}} \\ \bar{J}_{ul} &= \frac{\Omega_\star}{4\pi} I_\nu^\star \, \alpha_0(\tau_{\rm L}^{\rm rad}, \tau_{\rm C}^{\rm rad}) \;=\; \frac{\Omega_\star}{4\pi} I_\nu^\star \int \phi(x) \, {\rm e}^{-\tau_{\rm C}^{\rm rad} - \tau_{\rm L}^{\rm rad}\phi(x)} \, dx \;=\; J_\nu^{\rm cont} P_{ul}^{\rm pump,old} \;, \end{aligned}$$

   and therefore $P_{ul}^{\rm pump} = \bar{J}_{ul}/J_\nu^{\rm cont} = \alpha_0(\tau_{\rm L}, \tau_{\rm C})/{\rm e}^{-\tau_{\rm C}} = P_{ul}^{\rm pump,old}(\tau_{\rm L})$ is correct in this case.

2. Considering the limiting case $\Omega_\star \to 0$, i.e. $\Omega_{\rm d}/(8\pi) = 1/2$, and assuming the escape is purely vertically upward (for instance, $\tau_{\rm C}^{\downarrow} \to \infty$ would ensure that) we have

$$P_{ul}^{\rm esc} \;=\; 1 - \frac{1}{2}\Big(\beta_2(\tau_{\rm L}^{\uparrow}, \tau_{\rm C}^{\uparrow})\Big) \;=\; 1 - \frac{1}{2}\int \phi(x) \, \frac{\tau_{\rm L}^{\uparrow}\phi(x)}{\tau_{\rm C}^{\uparrow} + \tau_{\rm L}^{\uparrow}\phi(x)} \, \Big(1 - E_2\big(\tau_{\rm C}^{\uparrow} + \tau_{\rm L}^{\uparrow}\phi(x)\big)\Big) \, dx \;.$$

   If we now ignore the escape being hindered by the continuum (i.e. assuming $\tau_{\rm C}^{\uparrow} = 0$) then

$$P_{ul}^{\rm esc} \;=\; 1 - \frac{1}{2}\int \phi(x) \, \Big(1 - E_2\big(\tau_{\rm L}^{\uparrow}\phi(x)\big)\Big) \, dx \;=\; \frac{1}{2}\int \phi(x) \; E_2\big(\tau_{\rm L}^{\uparrow}\phi(x)\big) \, dx \;=\; P_{ul}^{\rm esc,old} \;.$$

These two cases can be used to check the numerical implementation of the new escape probability method in ProDiMo.

Figure 1 shows a comparison between old and new escape and pumping probabilities.

- The figue reveals some artefacts of the old treatment. Why should the pumping be always radial?
- The results of the new treatment show larger escape and pumping probabilities in general.

Figure 2 shows the resulting heating and cooling in the innermost 10 AU in the disk (T Tauri standard model). There are two significant changes:

- In the regions inside of 1 au which are borderline optically thin, relevant for the IR line emission, we find much increased H_2O heating and cooling rates, whereas previously there was a balance between UV driven heating by H_2 formation versus H_2O cooling. This is due to the very much increaed pumping and escape probabilities in these regions.
- Thermal accomodation in the midplane is now quite unimportant for both heating and cooling, unless the midplane becomes virtually molecule-free due to ice formation. In the optically thick midplane, dust and gas now exchange energy very efficiently via line photons, more efficiently than by inelastic collisions. And since the formulation of the line heating/cooling in ProDiMo is robust including all reverse processes and stimulated emission, $J_\nu^{\rm cont} = B_\nu(T_{\rm d})$ implies that a balance between line heating and cooling can only be achieved when $T_{\rm g} = T_{\rm d}$.

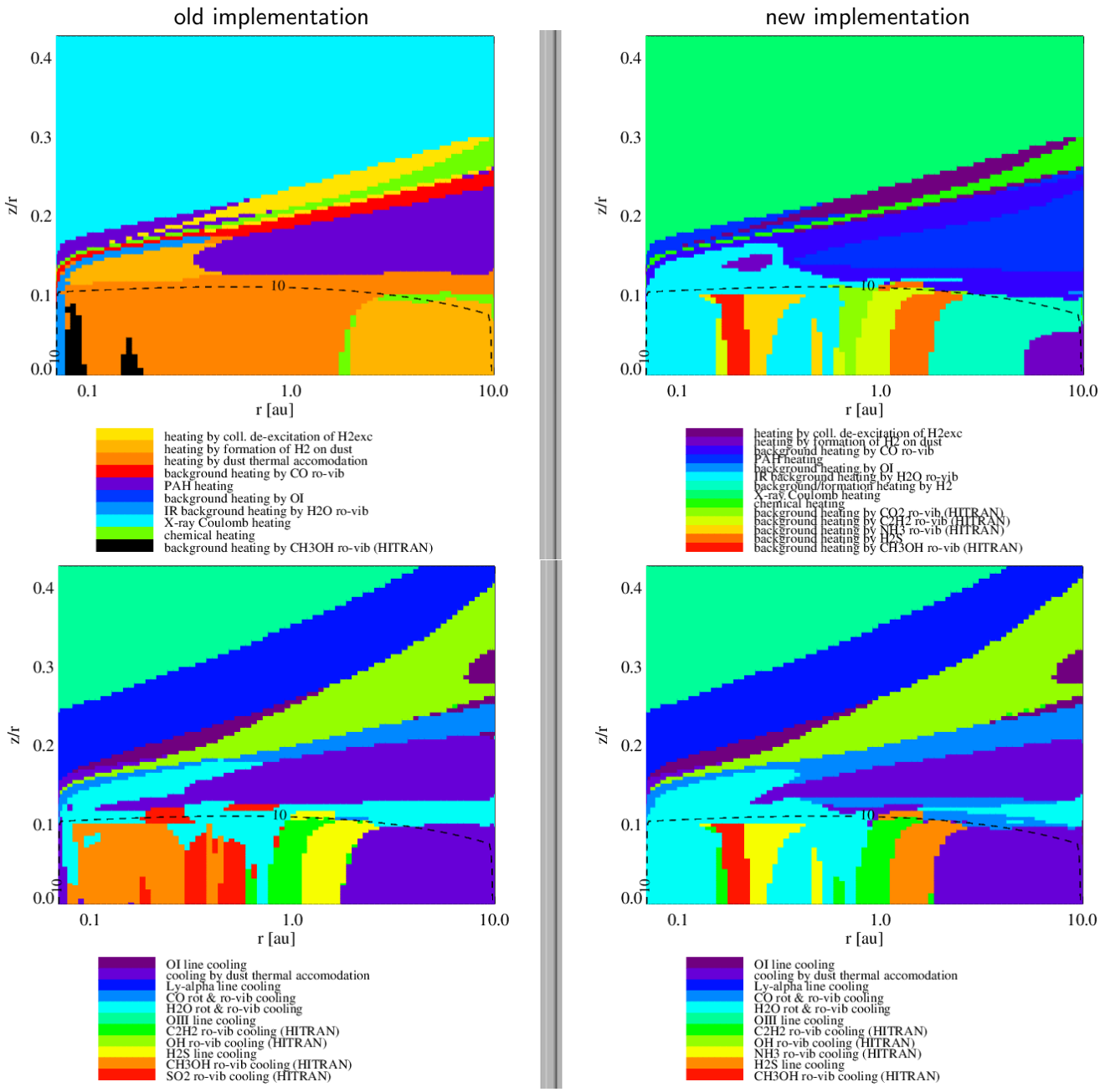

Figure 2: Change of heating/cooling with new escape probability treatment.

2 New escape probabilty treatment for line fluxes

In ProDiMo, line fluxes are estimated by using the escape probabilities, and then summing up the contributions from all cells. The following expression is used to calculate the luminosity [erg/s] of photon energy escaping in form of line photons from a single cell in the model

$$L^{\rm cell} = \Delta V\, n_{\rm u} A_{\rm ul}\, h\nu_{\rm ul} \int \phi(x)\, {\rm e}^{-\tau_{\rm L}\phi(x)-\tau_{\rm C}}\, dx \ , \tag{35}$$

where ΔV [cm^{-3}] is the volume of a cell k centered around point grid point (ix, iz). The line flux [erg/s/cm^2] is then calculated as

$$F_{\rm line} = \frac{\sum_k L_k^{\rm cell}}{4\pi d^2} \ , \tag{36}$$

where d is the distance to the object. We consider the vertical escape here (face-on disk), so the line and continuum optical depths are $\tau_{\rm L} = \tau_{\rm L}^{\uparrow}$ and $\tau_{\rm C} = \tau_{\rm C}^{\uparrow}$. Using the definition of the line emission coefficient, we have $n_{\rm u}A_{\rm ul}h\nu_{\rm ul} = 4\pi\kappa_{\rm L}S_{\rm L}$, and we can express the line luminosity of a cell, according to the old implementation, by

$$L^{\rm cell} = 4\pi\, \Delta V\, \kappa_{\rm L} S_{\rm L}\, {\rm e}^{-\tau_{\rm C}} \int \phi(x)\, {\rm e}^{-\tau_{\rm L}\phi(x)}\, dx \ . \tag{37}$$

This result corresponds to the case of a cold background $S_{\rm C} = 0$, expressed by the area **A** in Fig. 3. However, the question arrises how the line fluxes are affected by continuum opacity in detail. This is not a simple superposition, as the sketch (d) in Fig 3 suggests, because the escaping continuum photons are partly blocked by line opacity. This is shown by the lower graph in case (b), before the escaping line photons can be added, resulting in the upper graph in case (b).

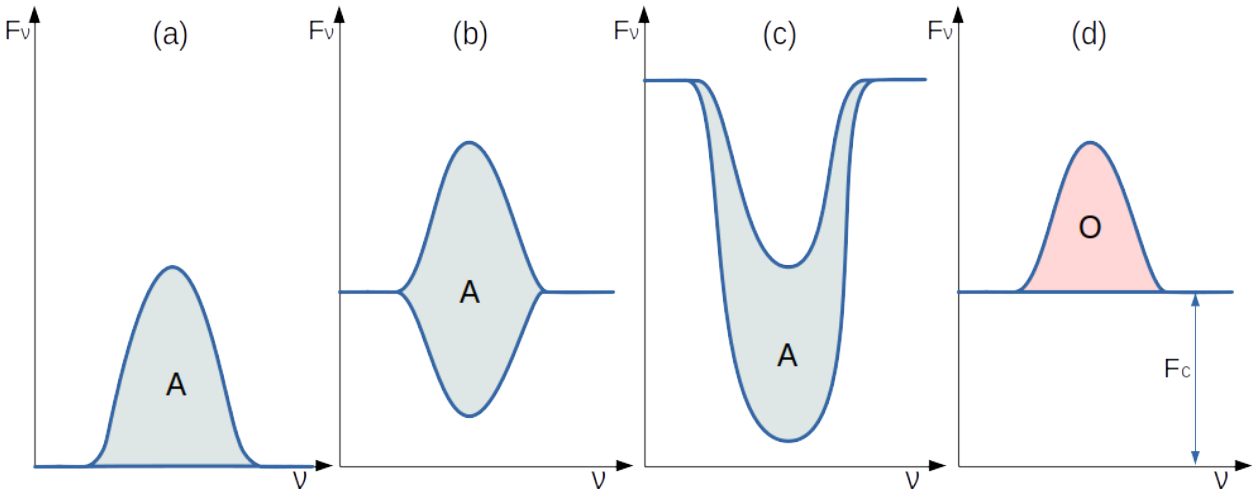

Figure 3: Effect of continuum emission on line flux. Case (a) shows an emission line on a cold continuum $S_{\rm C} = 0$. Case (b) is an emission line on a warm continuum $S_{\rm L} > S_{\rm C}$, and case (c) is an absorption line where the continuum is hot $S_{\rm L} < S_{\rm C}$. The area **A** is the flux of photon energy [erg/s/cm^2] carried away by line photons escaping vertically from the object (after continuum extinction and line self-absorption) and is the same in cases (a), (b) and (c). The task, however, is to derive the area **O**, which is the line flux as measured by observers. For a warm continuum, clearly $\mathbf{O} < \mathbf{A}$, and for an absorption line $\mathbf{O} < \mathbf{0}$ (although $\mathbf{A} > \mathbf{0}$).

In a more detailed model, we need compute the upper graph in case (b) and the pure continuum, and then subtract the two to simulate the way line fluxes are measured:

$$\text{without cont. (A)} \qquad L^{\rm cell} = 4\pi\,\Delta V \int \kappa_{\rm L} S_{\rm L} \phi_\nu \, {\rm e}^{-\tau_{\rm L}\phi(x)-\tau_{\rm C}}\, d\nu \;, \tag{38}$$

$$\text{with continuum} \qquad L^{\rm cell} = 4\pi\,\Delta V \int (\kappa_{\rm L} S_{\rm L} \phi_\nu + \kappa_{\rm C} S_{\rm C}) \, {\rm e}^{-\tau_{\rm L}\phi(x)-\tau_{\rm C}}\, d\nu \;, \tag{39}$$

$$\text{only continuum} \qquad L^{\rm cell} = 4\pi\,\Delta V \int \kappa_{\rm C} S_{\rm C} \, {\rm e}^{-\tau_{\rm C}}\, d\nu \;, \tag{40}$$

$$\text{cont. subtracted (O)} \qquad L^{\rm cell} = 4\pi\,\Delta V \, {\rm e}^{-\tau_{\rm C}}$$
$$\times \left(\kappa_{\rm L} S_{\rm L} \underbrace{\int \phi(x)\, {\rm e}^{-\tau_{\rm L}\phi(x)}\, dx}_{C_1(\tau_{\rm L})} \;-\; \kappa_{\rm C} S_{\rm C} \Delta\nu_{\rm D} \underbrace{\int \left(1 - {\rm e}^{-\tau_{\rm L}\phi(x)}\right) dx}_{C_2(\tau_{\rm L})} \right) \;. \tag{41}$$

Equation (41) shows that there is an additional correction term with respect to the old way of calculating the escaping line luminosity from a cell (Eq. 37). This new term describes the loss of continnum flux due to line absorption. The integration boundaries in these equations go from $-\infty$ to $+\infty$, so both intermediate results (Eqs. 39 and 40) are infinite, but the subtraction of the two is finite, following the observer's procedure how to measure a line flux. The function $C_1(\tau_{\rm L})$ describes the probability of an outgoing line photon not to be re-absorbed in the line again, and $C_2(\tau_{\rm L})$ describes the reduction of continuum photons escaping the object due to line opacity. The two functions $C_1(\tau_{\rm L})$ and $C_2(\tau_{\rm L})$ are plotted in Fig. 4.

According to this new formulation of escape probability, the line flux is *always smaller* when continuum emission effects are included, and can become negative when the continnum source function $S_{\rm C}$ is as large as the line source function $S_{\rm L}$.

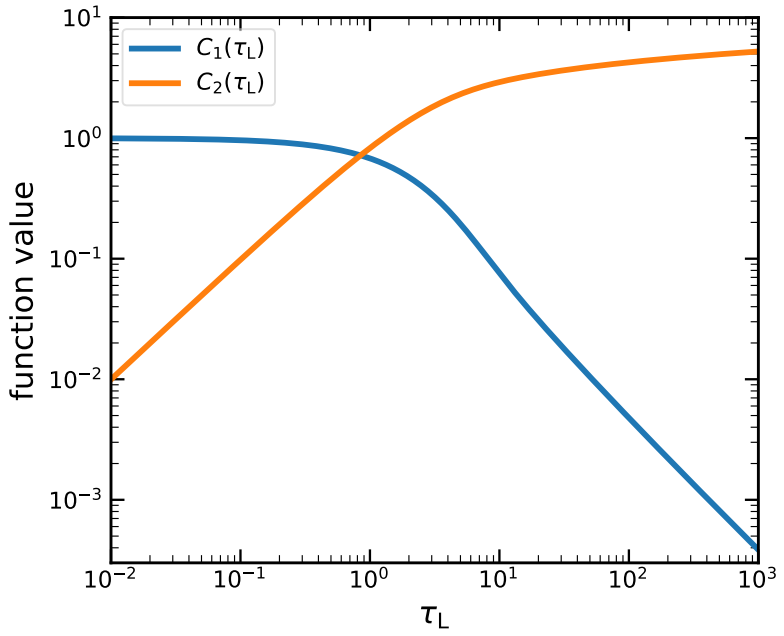

Figure 4: The functions $C_1(\tau_{\rm L})$ and $C_2(\tau_{\rm L})$ as introduced in Eq. (41).

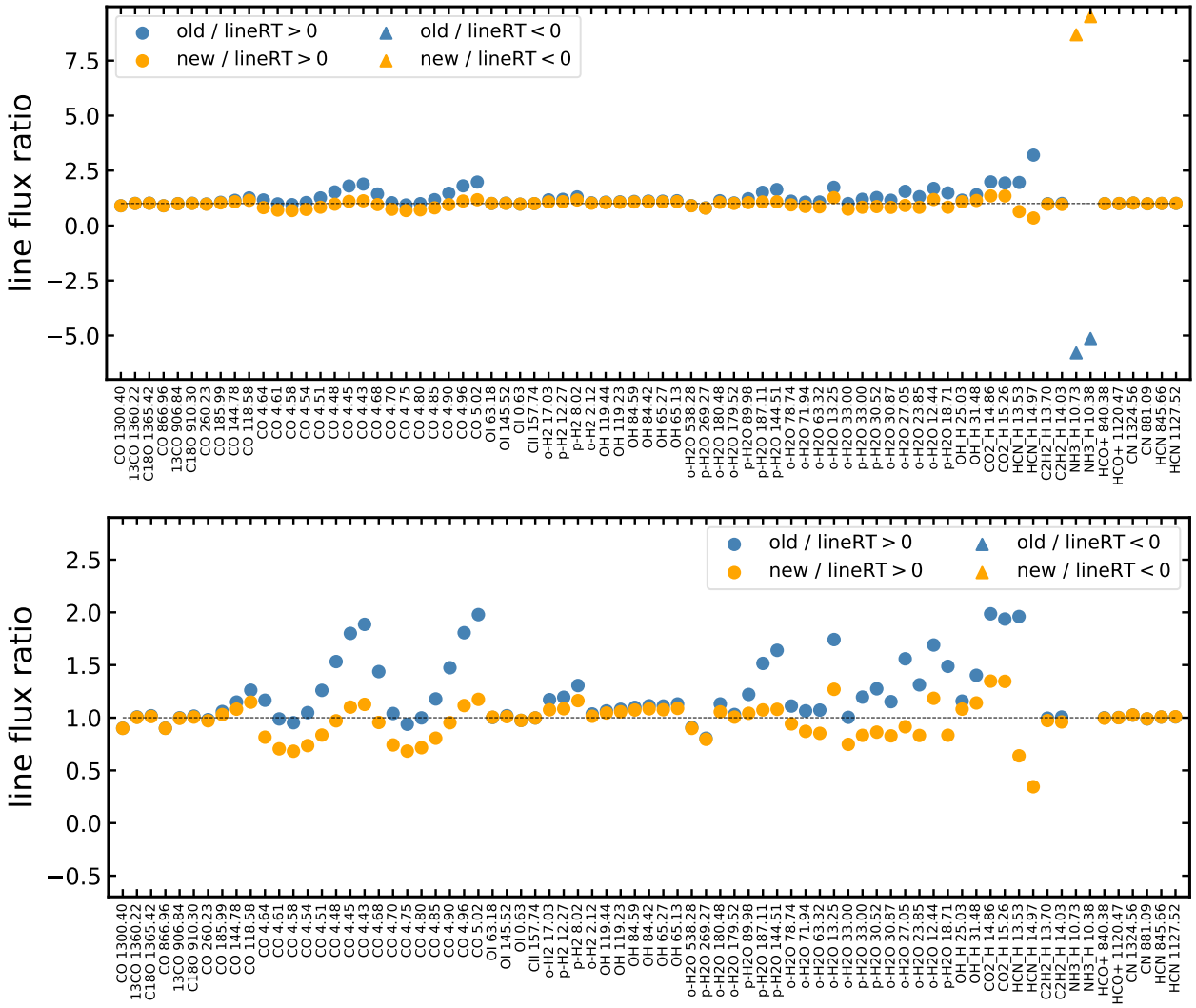

Figure 5: Line fluxes predicted by the old escape probability treatment (blue) and new escape probability treatment (orange) divided by the results from the proper line RT. The lower figure shows an enlargement of the same data.

3 New Treatment of 2D Molecular Shielding

Equation (28) offers a new way to tackle the problem of molecular shielding in 2D disk geometry. The shielding factors are used in ProDiMo to reduce the molecular photo-dissociation rates

$$R_{\rm ph} = 4\pi \int \sigma_{\rm ph}(\nu) \frac{J_\nu}{h\nu}\, d\nu \tag{42}$$

where $\sigma_{\rm ph}(\nu)$ is the local photo-dissociation cross section and J_ν is the local mean intensity. Without molecular shielding, we have $J_\nu = J_\nu^{\rm cont}$, where $J_\nu^{\rm cont}$ is the result from the continuum radiative transfer (RT). However, the UV molecular (line and continuous) opacities are not included in the dust continuum RT. They generally cause $J_\nu < J_\nu^{\rm cont}$, because there is no molecular UV emission, and hence these opacities reduce the photo rates.

This effect is currently taken into account in ProDiMo with different options. We differentiate between self-shielding and shielding. The former is particularly effective, because the absorbing lines are perfectly matching the lines causing the photo-dissociation. By default in ProDiMo, we have

- self-shielding C $\rightarrow$ C
- self-shielding $H_2 \rightarrow H_2$
- self-shielding CO $\rightarrow$ CO
- self-shielding $N_2 \rightarrow N_2$
- shielding C $\rightarrow H_2$
- shielding $H_2 \rightarrow$ C and $H_2 \rightarrow$ CO

In addition, there are a number of additional flags, including

- `C_shielding`: C $\rightarrow$ all
- `H2_shielding`: $H_2 \rightarrow$ all
- `self_shielding`: i $\rightarrow$ i for all molecules i.

In most of these cases, the shielding-factors are taken from detailed alien 1D models (semi-infinite slab), which resolved the UV lines and have published efficiency factors as function of column density of the molecular absorber "towards the source" and (local) temperature.

$$s_{i\rightarrow j} = s_{i\rightarrow j}(N_i, T_{\rm g}) \quad \text{with} \quad N_i = \int n(i)\, ds \tag{43}$$

For example, in the most straightforward case of shielding by neutral C-atoms with a constant continuous opacity, we have

$$J_\nu = J_\nu^{\rm cont}\, {\rm e}^{-\sigma_{\rm C} N_{\rm C}} \tag{44}$$

with constant cross section $\sigma_{\rm C} = 1.1 \times 10^{-17}\,{\rm cm}^2$, applied when $\lambda < 1100\,$Å. In more complicated cases, the line overlaps between shielding molecule and target molecule need to be assessed, and this depends on line broadening and hence on gas temperature. In general, the shielding factors can be applied one after the other, since $\exp(-\tau_{{\rm all}\rightarrow j}) = \exp\big(-\sum_i \sigma_{\rm i}(\nu) N_i\big) = \Pi_i \exp(-\sigma_{\rm i}(\nu) N_i)$.

The question now arrises how to deal with this problem in 2D. Which column density N_i is to be considered? The radial one, the vertically upward one, a mixture, or something else? Equation (28) holds an answer to that question. Using the explicit shapes of α_0, β_0 and β_1 for $\tau_{\rm L} \rightarrow 0$, and neglecting the α_1 term, which is the continuum emission of the disk in the solid angle of the star that is usually very small, this equation reads

$$J_\nu^{\rm cont} \;=\; \frac{\Omega_\star}{4\pi} I_\nu^\star\, {\rm e}^{-\tau_{\rm C}^{\rm rad}} \;+\; \frac{\Omega_{\rm d}}{8\pi} I_\nu^{\rm ISM} \Big(E_2(\tau_{\rm C}^{\uparrow}) + E_2(\tau_{\rm C}^{\downarrow}) \Big) \;+\; \frac{\Omega_{\rm d}}{8\pi} S_{\rm C} \Big(2 - E_2(\tau_{\rm C}^{\uparrow}) - E_2(\tau_{\rm C}^{\downarrow}) \Big) \tag{45}$$

Equation (45) states the influence of the three principle sources (the star, the ISM background, and the disk itself) on the calculated $J_\nu^{\rm cont}$. In the UV, there is no disk emission, but $S_{\rm C}$ contains

the continuum scattering. Clearly, if direct illumination from the star dominates, then $J_\nu^{\rm cont} \approx \frac{\Omega_\star}{4\pi} I_\nu^\star \, {\rm e}^{-\tau_{\rm C}^{\rm rad}}$ and one should use the radial column densities towards the star to compute the shielding factors. If interstellar UV irradiation dominates, one should take the vertical column densities. However, in the most interesting regions where we find a "warm molecular chemistry", none of these two terms is actually the important one, but it is the downward scattering of star light by the dust in the disk's upper layers, i.e. the third term is leading in Eq. (45)!

Now, if the third term actually dominates in Eq. (45), then it is clear that neither using the radial $N_i^{\rm rad}$ nor the vertical $N_i^{\rm ver}$ column densities is correct, as the light comes from relatively close-by. In the optically thick case, for example, we have ${\rm e}^{-\tau_{\rm C}^{\rm rad}} \rightarrow 0$, $E_2(\tau_{\rm C}^\uparrow) \rightarrow 0$ and $E_2(\tau_{\rm C}^\downarrow) \rightarrow 0$, so $J_\nu^{\rm cont} \approx S_{\rm C} \frac{\Omega_{\rm d}}{4\pi} \approx S_{\rm C}$.

3.1 The old 2D treatment of shielding

Currently, we use dust optical depths $\tau_{\rm C}^{\rm rad}$ and $\tau_{\rm C}^\uparrow$, frequency-averaged over the Draine UV-band, to calculate weighting factors

$$
\begin{aligned}
J_{\nu,{\rm rad}}^{\rm cont} &= \frac{\Omega_\star}{4\pi} I_\nu^\star \, {\rm e}^{-\tau_{\rm C}^{\rm rad}} && (46)\\
J_{\nu,{\rm ver}}^{\rm cont} &= I_\nu^{\rm ISM} E_2(\tau_{\rm C}^\uparrow) && (47)\\
w_{\rm rad} &= \frac{J_{\nu,{\rm rad}}^{\rm cont}}{J_{\nu,{\rm rad}}^{\rm cont} + J_{\nu,{\rm ver}}^{\rm cont}} && (48)\\
w_{\rm vert} &= \frac{J_{\nu,{\rm ver}}^{\rm cont}}{J_{\nu,{\rm rad}}^{\rm cont} + J_{\nu,{\rm ver}}^{\rm cont}} && (49)\\
s_{i\rightarrow j} &= w_{\rm rad} \, s_{i\rightarrow j}(N_i^{\rm rad}, T_{\rm g}) \; + \; w_{\rm vert} \, s_{i\rightarrow j}(N_i^\uparrow, T_{\rm g}) && (50)\\
J_\nu &= s_{i\rightarrow j} \, J_\nu^{\rm cont} && (51)
\end{aligned}
$$

where $w_{\rm rad}$ and $w_{\rm vert}$ are the radial and vertical weights, using the idea to assess what's more important, the direct stellar illumination or the vertical illumination? But this is obviously a very rough assumption, as the often most important source (the third term in Eq. 45) is not even considered here, and thus $J_\nu^{\rm cont} \gg J_\nu^{\rm rad} + J_\nu^{\rm vert}$. Instead, based on the mixing ratio between $J_\nu^{\rm rad}$ and $J_\nu^{\rm vert}$, an efective shielding factor is created which is applied to all of $J_\nu^{\rm cont}$.

3.2 The new 2D treatment of shielding

It is noteworthy that whatever we do here will be very approximate, as for a proper 2D treatment we would need to have a UV line-resolved 2D radiative transfer including detailed molecular UV opacities and dust scattering, which we do not.

Contrary to the IR pumping of molecules, which often comes from the warm dust below the point of interest, the UV radiation mainly arrives from two directions, the direct radial and the vertically downward directions. Here, "vertically downward" should include the diffuse scattering term containing $S_{\rm C}$ in Eq. (45). The effect of molecular shielding on that diffuse part of $J_\nu^{\rm cont}$ is difficult to assess, as we would need to know the *molecular column density along the scattered photon path*. But given a choice between radial and vertical column density, chosing the vertical one seems more appropriate. In that case we have

$$
\begin{aligned}
J_{\nu,{\rm rad}}^{\rm cont} &= \frac{\Omega_\star}{4\pi} I_\nu^\star \, {\rm e}^{-\tau_{\rm C}^{\rm rad}} && (52)\\
J_{\nu,{\rm ver}}^{\rm cont} &= J_\nu^{\rm cont} - J_{\nu,{\rm rad}}^{\rm cont} && (53)\\
J_\nu &= s_{i\rightarrow j}(N_i^{\rm rad}, T_{\rm g}) \, J_{\nu,{\rm rad}}^{\rm cont} \; + \; s_{i\rightarrow j}(N_i^{\rm ver}, T_{\rm g}) \, J_{\nu,{\rm vert}}^{\rm cont} && (54)
\end{aligned}
$$

The difference to the old treatment lies in Eq. (47), which is questionable. It seems better to include the diffuse scattering part of $J_\nu^{\rm cont}$ containing $S_{\rm C}$ by using Eq. (53), assuming that the scattered star light mainly comes from above.

Since we ignore the diffuse scattering in the old treatment, the old vertical part $J_{\nu,\rm ver}^{\rm cont}$ is too small, and hence we switch from radial to vertical column densities too late, i.e. *we currently overestimate the effects of molecular shielding.*

Figure 6 shows that, as expected, the formation of CO happens now slightly deeper in the disk. The feedback on more complex molecules like HCN and C_2H_2 is remarkable, leading to profoundly changed conditions for the emission of molecular IR lines. The formation of these molecules is triggered by neutral carbon atoms, which are now also sitting slightly deeper in the disk, i.e. at larger densities, which seems to favour the formation of the more complex molecules.

3.3 Parametric photorates

One remaining problem is how to deal with the photorates where we don't have detailed cross sections but only the reaction coefficients α, γ for the formula $R_{\rm ph} = \chi\,\alpha\,\exp(-\gamma A_V)$. In such cases, ProDiMo defines a "generic" cross section

$$\sigma^{\rm ph}(\lambda) = \sigma_0 \exp\left(-\left(\frac{\lambda_0 - \lambda}{\Delta\lambda}\right)^2\right) \tag{55}$$

with two parameters σ_0 and λ_0, assuming $\Delta\lambda = 0.1\,\lambda_0$. These two parameters are then fitted for each molecule to the given α, γ parameters. Precisely speaking, two $R_{\rm ph}$ are generated, for $A_V = 0$ and $A_V = 0.5$, and then σ_0 and λ_0 are varied until a perfect fit is achieved for a standard Draine UV field attenuated by standard ISM dust properties. In the disk model, the photorate is then computed as usual

$$R_{\rm ph} = \frac{1}{h}\int \sigma^{\rm ph}(\lambda)\,\lambda u_\lambda\,d\lambda \tag{56}$$

where $\lambda u_\lambda = J_\lambda^{\rm cont}\,4\pi/c$ is taken from the continuous radiative transfer.

So far, no molecular shielding factors were applied to these photorates. However, with the new implementation, we also include them in a very straightforward way, in routine `GET_PHOTORATE()`,

$$J_\nu = s_{i\to j}(N_i^{\rm rad}, T_{\rm g})\,J_{\nu,\rm rad}^{\rm cont} \;+\; s_{i\to j}(N_i^{\rm ver}, T_{\rm g})\,J_{\nu,\rm vert}^{\rm cont} \tag{57}$$

using the concepts to separate $J_\nu^{\rm cont}$ into $J_{\nu,\rm rad}^{\rm cont}$ and $J_{\nu,\rm vert}^{\rm cont}$ as explained in Sects. 3.1 and 3.2. If the underlying molecular (line) opacity is all but smooth, Eq. (**??**) should underestimate the self-shielding effects, but never over-estimate.

A remaining complication is that some additional photorates of processes like S6-surface reactions, PAHs photoionisation, etc., and the most important photo processes of H_2, CO and C, are handled in various approximations elsewhere in the code. I struggeled a lot with cases where $R_{\rm ph} = \chi\,\alpha\,\exp(-\gamma A_V)$ is explicitly used, which should be avoided at all costs. I think it is all good now, but this is hard to test.

Peter Woitke, December 12, 2022

References

Hummer, D. G., Rybicki, G. B. (1985, June). The Sobolev approximation for line formation with continuous opacity. *ApJ* **293**, 258–267.

Woitke, P., Kamp, I., Thi, W. F. (2009, July). Radiation thermo-chemical models of protoplanetary disks. I. Hydrostatic disk structure and inner rim. *A&A* **501**(1), 383–406.

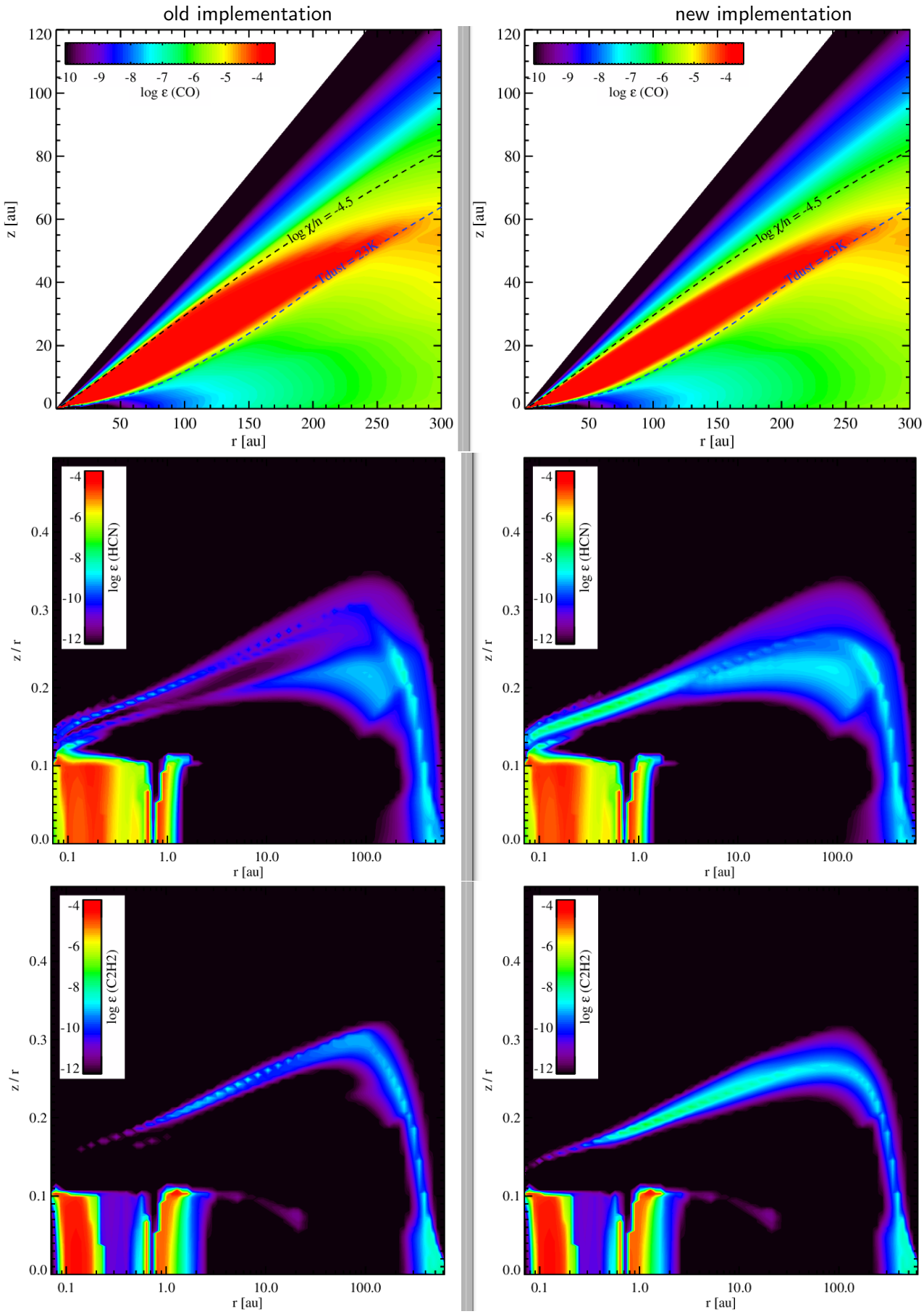

Figure 6: Change of molecular concentrations with the new 2D concept of applying the same radial and vertical molecular shielding factors.